# Modality-Augmented Fine-Tuning of Foundation Robot Policies for Cross-Embodiment Manipulation on GR1 and G1

Junsung Park<sup>1</sup>, Hogun Kee<sup>1</sup>, and Songhwai Oh<sup>1</sup>

<sup>1</sup>Department of Electrical and Computer Engineering, Seoul National University

Abstract—We present a modality-augmented fine-tuning framework for adapting foundation robot policies to diverse embodiments. Our study evaluates two settings: (i) the GR1 embodiment using the public HuggingFace dataset, where we introduce post-processed modalities including binary contact signals and ZoeDepth-generated metric depth; and (ii) the Unitree G1 embodiment, for which we build a new multi-modal dataset using cuRobo motion planning, inverse kinematics, and ground-truth contact-force measurements (HuggingFace repository).

Modality augmentation consistently improves policy performance across embodiments. On GR1, adding contact-state cues and RGB-D fusion increases online success from 51% to 63%. On the G1 *Pick Apple to Bowl* task, zero-shot GR00T achieves 0% success, standard fine-tuning reaches 48%, and our contact-enhanced model attains up to 94%.

Overall, our results show that lightweight post-processing strengthens GR1 policies, while high-quality multi-modal data enables reliable Unitree G1 embodiment transfer. This work demonstrates a unified, data-centric pathway for extending foundation robot policies through targeted modality design and multi-modal fine-tuning.

# I. INTRODUCTION

Recent advances in foundation robot policies have demonstrated that large-scale, vision-language-action (VLA) models such as Isaac GR00T N1.5 [9] and PiZero can serve as strong generalist controllers capable of performing diverse manipulation tasks. These models leverage massive demonstration datasets and diffusion-based action generation [1], [2], [3], enabling robust trajectory synthesis and long-horizon control. However, despite these successes, current foundation policies still exhibit notable limitations when deployed in fine-grained manipulation settings that require accurate perception of contact events, reliable depth reasoning, and precise interaction-aware control.

As highlighted in the GR00T N1 report [9], existing robotic datasets form an archipelago of "data islands" arising from heterogeneous embodiments, sensing configurations, and control modes. This heterogeneity prevents foundation models from leveraging Internet-scale data in the same way as language or vision models. Moreover, cross-embodiment generalization remains challenging because robot morphology and kinematic structure fundamentally shape the distribution of feasible motions and interaction strategies. While GR00T addresses part of this challenge through embodiment-specific encoders and a dual-system architecture, its generalization ability is ultimately bounded by the modalities present in its training data.

A concrete example of these modality limitations appears in the publicly available GR1 dataset on HuggingFace, which provides RGB observations and proprioceptive states but lacks key interaction-centric modalities such as depth, binary contact indicators, or force measurements. Without these modalities, VLA models must infer contact and object interaction boundaries purely from color imagery—an ill-posed problem in scenarios involving occlusion, object overlap, or visually ambiguous contact transitions. As a result, GR00T-style policies often struggle to detect stable grasps, reason about object-robot contact timing, or maintain closed-loop stability during contact-rich manipulation. These limitations become even more pronounced when transferring a foundation model to a new embodiment such as the Unitree G1, where differences in kinematics, actuation, workspace geometry, and camera placement further degrade zero-shot performance.

To address these limitations, we adopt a data-centric and modality-augmented fine-tuning strategy. For the GR1 embodiment, we enrich the original dataset by post-processing demonstrations to estimate metric depth via ZoeDepth and by injecting binary contact signals derived from collision reasoning within the simulator. This yields a multi-modal variant of the GR1 dataset suitable for training policies that better understand object interaction boundaries. For the G1 embodiment—where no public dataset exists—we generate a fully customized multi-modal demonstration set using cuRobo-based motion planning and inverse kinematics [17]. This pipeline provides precise trajectories paired with ground-truth contact force measurements, enabling us to analyze how modality composition and embodiment-specific data influence policy adaptation.

Our contributions are threefold. (1) We construct multimodal GR1 and G1 datasets that incorporate depth and contact information, addressing the modality bottlenecks that limit current VLA foundation policies. (2) We propose lightweight architectural augmentations for incorporating contact and depth signals into the GR00T diffusion policy without modifying the core model structure. (3) We demonstrate that modality-augmented fine-tuning substantially improves manipulation success rates and enables strong embodiment transfer from GR1 to G1, reducing the performance gap introduced by morphological differences.

Overall, this work presents a practical pathway for adapting foundation robot policies to new embodiments and interaction-rich tasks by explicitly engineering the sensory

modalities that underpin robust manipulation.

#### II. PRELIMINARIES

### A. Diffusion Policy

Diffusion policy is a generative action model that formulates robot control as a conditional denoising process. Instead of predicting actions directly, the policy learns a diffusion model that iteratively transforms a noisy latent action representation into a feasible trajectory conditioned on observations. This formulation is grounded in denoising diffusion probabilistic models [1] and their implicit variants [2], and has recently been extended to Transformer-based architectures such as DiT [3].

Formally, let  $\mathbf{o}_t$  denote the observation at time t, including proprioceptive states or visual features, and let  $\mathbf{a}_{t:t+H}$  represent a future action sequence over a horizon H. The diffusion policy samples a noisy latent  $\mathbf{x}_T$  from a Gaussian prior and gradually denoises it over T steps using a learned denoising network  $\epsilon_\theta$ :

$$\mathbf{x}_{t-1} = \frac{1}{\sqrt{\alpha_t}} \left( \mathbf{x}_t - \frac{1 - \alpha_t}{\sqrt{1 - \bar{\alpha}_t}} \epsilon_{\theta}(\mathbf{x}_t, \mathbf{o}_t) \right) + \sigma_t \mathbf{z}.$$

Here,  $\alpha_t$  and  $\sigma_t$  follow a predefined noise schedule, and **z** is Gaussian noise. After the final denoising step, the clean latent  $\mathbf{x}_0$  is decoded into an action sequence via

$$\mathbf{a}_{t:t+H} = f_{\theta}(\mathbf{x}_0).$$

Replacing the traditional UNet with a Transformer backbone—as done in DiT and subsequent robotic diffusion policies—enables scalability and improves multimodal conditioning. This approach provides two key advantages for robot manipulation: (1) *Multimodality*: the policy can generate diverse yet valid action trajectories under ambiguous perception, and (2) *Temporal coherence*: predicting full action sequences improves stability for long-horizon tasks.

## B. Isaac GR00T

Isaac GR00T is an open Vision-Language-Action (VLA) foundation model designed for general-purpose humanoid robotics [9]. As illustrated in Fig. 1, GR00T adopts a dual-system cognitive architecture inspired by human System 1 and System 2 processing. System 2 is a Vision-Language Model (VLM) that interprets instructions and visual observations, while System 1 is a Diffusion Transformer (DiT) that performs low-level motor action generation.

The VLM encodes RGB images into visual tokens and tokenizes language instructions into text tokens, providing semantic grounding of the task objective and object relationships. In parallel, the robot's proprioceptive state is embedded into state tokens through embodiment-specific encoders. All tokens are then passed to the DiT module, which applies the diffusion-based action generation described in Sec. II-A using transformer-based denoising rather than a UNet. This enables improved scalability, conditioning, and data efficiency.

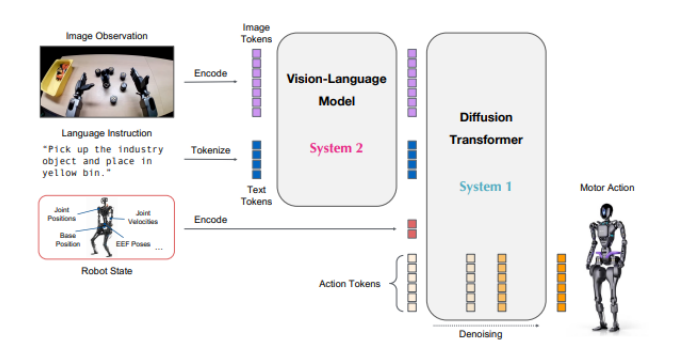


Fig. 1. Overview of the GR00T dual-system architecture. System 2 (VLM) processes image observations and language instructions into semantic tokens, while System 1 (Diffusion Transformer) generates motor actions via iterative denoising conditioned on multimodal tokens.

A central design goal of GR00T is embodiment generality. State and action projection layers embed each robot's observation and action space into a unified token dimension, allowing the same diffusion policy to be fine-tuned across heterogeneous embodiments such as the Fourier GR1 or the Unitree G1. This provides a strong foundation for building manipulation policies, while still allowing additional modalities such as depth or contact to be incorporated during fine-tuning.

In this work, GR00T serves as the base policy for modality augmentation. By enriching the GR1 dataset with post-processed depth and contact estimates, and by constructing a fully multi-modal G1 dataset that includes contact force measurements, we investigate how GR00T's diffusion-based architecture adapts to richer sensory inputs and transfers across embodiments.

# III. PROBLEM FORMULATION

### A. Task Definition

We consider two robot embodiments: the Fourier GR1 and the Unitree G1. For the GR1 platform, we use three manipulation tasks from the publicly available GR1 dataset on HuggingFace: (1) *Pick-and-Place Can to Drawer Close*, (2) *Pick-and-Place Potato to Microwave Close*, and (3) *Pick-and-Place Wine to Cabinet Close*. Each task requires long-horizon manipulation with object interaction, container insertion, and precise end-effector control.

For the G1 embodiment, no public dataset exists; therefore, we focus on a single custom-defined task, *Pick Apple to Bowl*, which requires stable grasp acquisition, object transport, and placement. This task allows us to evaluate embodiment adaptation under newly collected multi-modal data.

#### B. Multi-Embodiment Policy Adaptation

Adapting a single foundation policy to both GR1 and G1 introduces two primary challenges.

Observation-space mismatch.: The GR1 dataset provides RGB images and proprioceptive states, but lacks depth, contact indicators, or force feedback. In contrast, the G1



Fig. 2. Visualization of the G1 data collection environment. Left: front view of the scene setup. Right: ego-centric view from the robot's onboard camera during demonstration execution.

dataset we construct includes RGB-D observations, proprioception, and ground-truth contact forces. As a result, the policy must operate under heterogeneous and embodiment-specific sensory modalities across the two platforms.

Action-space mismatch.: Beyond sensory differences, the two robots differ significantly in embodiment. The GR1 platform uses a Fourier hand with 6 DoF, paired with a 7-DoF arm (13 DoF per arm, 26 DoF for both upper limbs), whereas the G1 platform employs a 7-DoF dexterous hand combined with a 7-DoF arm (14 DoF per arm, 28 DoF total). These differences in hand kinematics, finger actuation, and joint coordination introduce a non-trivial embodiment gap, raising the question of whether a single diffusion-based policy can transfer effectively across robots whose gripper morphology and manipulability differ substantially.

### C. Objective

Our goal is to enable a single diffusion-based policy to operate robustly across two robot embodiments with heterogeneous sensing and action modalities. To this end, we consider two complementary datasets: (i) an RGB-only GR1 dataset that we augment with estimated depth maps and binary contact indicators, and (ii) a custom multi-modal G1 dataset that includes RGB-D observations, proprioception, cuRobo-generated reference trajectories, and ground-truth contact-force measurements.

The objective is to fine-tune a unified policy that can:

- perform stable and contact-aware manipulation by leveraging richer sensory modalities, and
- transfer effectively across robots with different embodiments, hand structures, and action spaces (GR1  $\rightarrow$  G1).

More formally, we aim to learn a policy  $\pi_{\theta}$  that generates action sequences via a diffusion denoising process while maintaining consistency and performance under variations in embodiment, sensing modality, and task specifications. The policy should generalize across both datasets and exploit modality augmentation to improve robustness in contact-rich manipulation scenarios.

#### IV. PROPOSED METHOD

# A. G1 Dataset Creation

Unlike the GR1 platform, no public dataset exists for the Unitree G1. Moreover, the G1 embodiment differs substantially in hand morphology (7-DoF dexterous hand) and

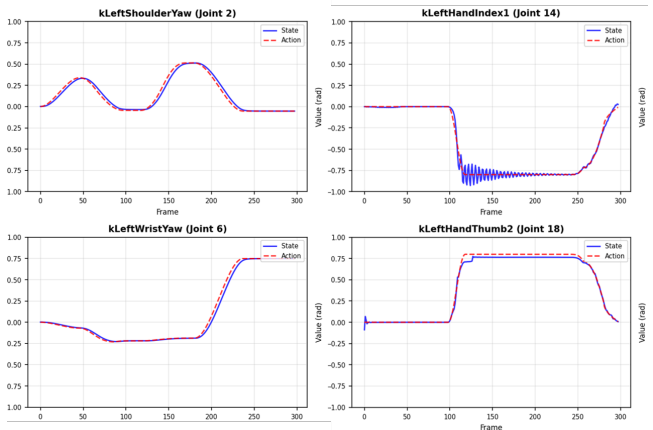


Fig. 3. **State vs. Action per G1 joint.** For each joint, we visualize the proprioceptive state (blue) and the executed action command (red) over time. The trajectories generated through cuRobo-based planning exhibit smooth, consistent evolution across the 20 DoF upper-limb chain, ensuring high-quality supervision for diffusion policy fine-tuning.

upper-limb kinematics (7-DoF arm), making direct transfer from GR1 challenging. To enable modality-augmented fine-tuning and embodiment evaluation, we construct a high-quality, multi-modal demonstration dataset for the *Pick Apple to Bowl* task using a motion-planning–driven pipeline.

Trajectory generation via cuRobo.: We leverage cuRobo's GPU-accelerated motion planner to generate smooth and collision-free end-effector trajectories. For each demonstration, cuRobo computes dynamically feasible Cartesian paths that satisfy grasping and placement constraints. These trajectories are converted to G1 joint-space commands using an analytical inverse kinematics (IK) solver, producing reference trajectories with high temporal consistency.

Proprioception and joint-action recording.: During trajectory rollout, we record the full proprioceptive state, including joint positions, joint velocities, and end-effector poses. We also log the executed joint actions generated by the controller at each timestep. Fig. 3 shows an example of the recorded state—action alignment across the 20 joints of the G1 upper-limb chain, demonstrating that the generated trajectories exhibit smooth and physically valid motion profiles.

Ground-truth contact force measurement.: A key feature of the G1 dataset is the availability of accurate contact-force feedback from the dexterous hand. For each frame, we extract fingertip and palm contact forces using the G1 physics engine. These signals allow the policy to learn fine-grained interaction cues such as grasp stability, slip, and object contact boundaries.

Fig. 4 illustrates the per-finger contact forces during a representative demonstration. The left thumb, left middle finger, and palm exhibit strong, temporally structured contact patterns during grasping, while other fingers remain inactive—highlighting the asymmetric force distribution characteristic of dexterous manipulation.

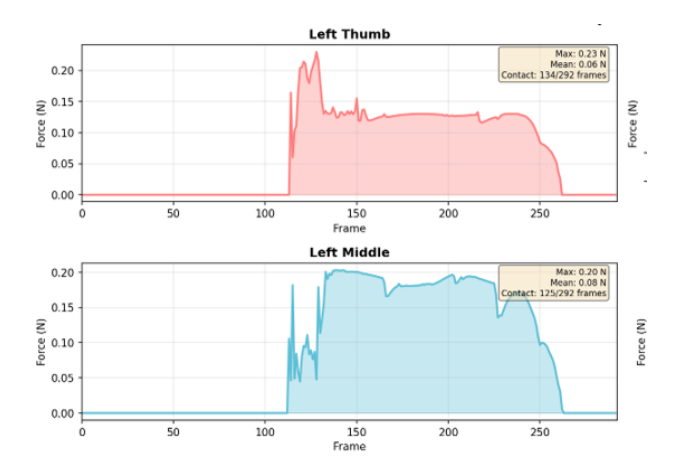


Fig. 4. Contact forces per finger over time. The G1 dexterous hand provides high-fidelity fingertip and palm force measurements. During grasp execution, contact is concentrated on specific fingers (left thumb, middle, and palm), while others remain inactive. These rich interaction signals are used to train contact-aware diffusion policies.

*Multi-modal observation structure.*: Each demonstration in the G1 dataset includes:

- RGB-D observations from the onboard camera,
- **full proprioception** (joint positions, velocities, end-effector pose),
- cuRobo-generated joint-space reference trajectories,
- fingertip and palm contact-force vectors.

This multi-modal dataset provides the dense physical and perceptual cues necessary for training policies capable of contact-rich manipulation and for evaluating cross-embodiment transfer from GR1 to G1.

### B. Contact Augmentation for GR1 Dataset

The GR1 dataset does not contain any contact information, preventing the policy from identifying grasp events, slip boundaries, or object—robot interaction timing. To compensate for this modality gap, we introduce two complementary forms of contact augmentation: (1) fusing collision-derived contact signals directly into the robot's proprioceptive state, and (2) treating contact as a distinct modality through a dedicated contact encoder.

1) Fusing Contact into Proprioceptive State: We first adopt a lightweight strategy that augments the GR1 proprioceptive state vector with a binary contact indicator. For each timestep, we detect collisions between the end-effector and the manipulated object in simulation and assign a 1-bit contact value  $c_t \in \{0,1\}$ , which is concatenated to the original state vector:

$$\tilde{s}_t = [s_t^{\text{joints}}, c_t].$$

This minimally increases the input dimension of the state encoder while allowing the diffusion policy to reason about object interaction boundaries. The augmented state is passed through the embodiment-specific state encoder to obtain a contact-aware embedding:

$$z_t = \operatorname{StateEnc}(\tilde{s}_t).$$

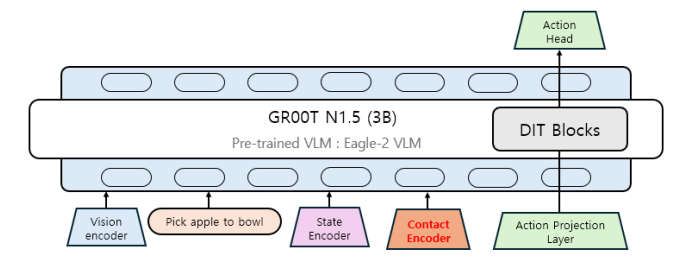


Fig. 5. **Dedicated Contact Encoder Module.** Instead of concatenating contact into the proprioceptive state, the binary (or continuous) contact signal  $c_t$  is processed by a learnable Contact Encoder. The resulting embedding is input to the DiT blocks as a separate modality, alongside vision, language, and state tokens. This design treats contact as an independent modality and allows the policy to learn richer interaction-aware representations.

During denoising, this embedding conditions the DiT backbone via cross-attention, directly influencing noise prediction:

$$x_{t-1} = \frac{1}{\sqrt{\alpha_t}} \left( x_t - \beta_t \, \epsilon_\theta(x_t, z_t, t) \right) + \sigma_t z,$$

where  $x_t$  is the noisy action,  $\epsilon_{\theta}$  is the DiT denoiser, and t is the diffusion step.

This simple augmentation provides a strong supervisory signal: contact-aware embeddings help the policy stabilize grasping actions, prevent premature release, and improve the consistency of object transport behaviors.

2) Dedicated Contact Encoder Module: To treat contact as an independent sensory modality rather than a scalar feature embedded into the proprioceptive state, we introduce a dedicated contact encoder module (Fig. 5). Here, the contact signal  $c_t$  is encoded through a learnable MLP before entering the diffusion transformer, allowing the model to represent interaction dynamics at a higher level of abstraction.

Formally, the contact embedding is obtained as:

$$z_t^{\text{contact}} = \text{ContactEnc}(c_t),$$

which captures temporal and semantic structure in the contact sequence. The full conditioning set for each DiT block becomes:

$$Z_t = \begin{bmatrix} z_t^{\text{vision}}, \ z_t^{\text{text}}, \ z_t^{\text{state}}, \ z_t^{\text{contact}} \end{bmatrix},$$

ensuring that contact is treated as a first-class modality, equal in importance to vision and proprioception.

By injecting contact as an independent token stream, the denoiser  $\epsilon_{\theta}$  gains explicit access to tactile cues during each diffusion step. This enables the model to differentiate between weak vs. strong grasp phases, detect pre-contact vs. post-contact transitions, and learn more expressive representations for contact-rich manipulation.

## C. Depth Augmentation (RGB-D Fusion)

The GR1 dataset contains only RGB observations, which restricts the policy's ability to reason about 3D geometry, object boundaries, and occlusions. To overcome this limitation, we generate metric depth maps for all GR1

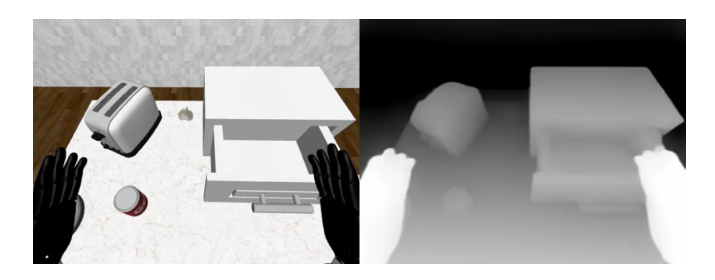


Fig. 6. RGB and Estimated Depth for GR1 Demonstrations. Left: original RGB observation from the GR1 simulator. Right: corresponding metric depth map computed by ZoeDepth. Depth enhances geometric reasoning by capturing spatial structure such as object shape, table height, and cabinet geometry.



Fig. 7. Example simulation environments used for online evaluation. Each rollout randomizes object placement, textures, lighting, and robot configuration to assess robustness.

demonstrations using ZoeDepth, a state-of-the-art monocular depth estimator capable of producing scale-consistent depth predictions. The resulting RGB-D frames equip the policy with explicit geometric cues that are essential for contact-rich manipulation.

Extending the Vision Encoder for RGB-D Input.: GR00T's Eagle-2 ViT processes  $16\times16$  RGB patches using a linear projection layer. To incorporate depth, we expand the patch embedding from 3 to 4 channels. For each  $16\times16$  patch  $P_t$  from the RGB-D input  $I_t\in\mathbb{R}^{H\times W\times 4}$ :

$$e_t = W_{\text{patch}} \cdot \text{Flatten}(P_t) + b_{\text{patch}},$$

with

$$W_{\text{patch}} \in \mathbb{R}^{d \times (16 \times 16 \times 4)}$$
.

To stabilize early training, the depth-channel weights are initialized using RGB kernel averaging:

$$W_{\mathrm{patch}}^{(D)} = \frac{1}{3} \left( W_{\mathrm{patch}}^{(R)} + W_{\mathrm{patch}}^{(G)} + W_{\mathrm{patch}}^{(B)} \right).$$

*RGB-D Token Fusion.*: The depth map is concatenated with the RGB channels prior to the Vision Encoder, forming an RGB-D input that undergoes early fusion through the expanded patch embedding layer. Once embedded, the RGB-D patches pass through the standard ViT encoder without architectural modification. The resulting tokens  $\{z_t^{\rm img}\}$  encode both appearance and geometric structure, enabling the diffusion policy to reason more effectively about depth discontinuities, grasp approach angles, and occluded object surfaces.

#### V. EXPERIMENTS

## A. Experimental Settings

Hardware and Environment.: All experiments are conducted on a single NVIDIA A6000 GPU using the official GR00T fine-tuning framework. Online evaluation is performed in a robosuite and robocasa based simulator via a server–client inference pipeline, while offline evaluation uses trajectory reconstruction MSE computed from the dataset.

Training Configuration.: We fine-tune the GR00T-N1.5-3B base model with the vision tower and VLM backbone frozen. Only the projector and embodiment-specific state/action encoders are updated. Training uses the AdamW optimizer with a learning rate of 1e-4, weight decay of 1e-5, cosine LR schedule with 5% warmup, and batch size 32. Models are trained for 20k steps using bf16 precision. Checkpoints are saved every 5,000 steps.

Diffusion and Policy Head.: Action generation uses GR00T's diffusion transformer with 12 layers, 8-head cross-attention, hidden size 1024, and GELU activation. Flow-matching training employs a Beta noise distribution ( $\alpha$ =1.5,  $\beta$ =1.0) with 1,000 timestep discretization.

#### B. Evaluation Protocol

We evaluate all models using two complementary procedures: (1) offline trajectory reconstruction and (2) online policy rollout in simulation. This dual protocol allows us to measure both the accuracy of the diffusion model's action prediction and its real-time manipulation capability.

Offline Evaluation (Trajectory MSE).: Given an observation sequence  $\mathbf{o}_t$  from the dataset, the diffusion policy predicts a 16-step action sequence  $\hat{\mathbf{a}}_{t:t+H}$  through iterative denoising. We compute the mean-squared error (MSE) between the predicted and ground-truth actions:

$$MSE = \frac{1}{H} \sum_{k=0}^{H-1} \|\hat{\mathbf{a}}_{t+k} - \mathbf{a}_{t+k}\|_{2}^{2}.$$

This metric quantifies the policy's ability to reconstruct expert trajectories and reflects the quality of multimodal conditioning (contact, depth, proprioception). Offline evaluation is performed on held-out validation data from both GR1 and G1 datasets.

Online Evaluation (Success Rate).: To evaluate real-time manipulation performance, we deploy the policy in a simulator stack composed of robosuite and robocasa. robosuite provides the manipulation task environments, while robocasa supplies object assets, scene setups, and interaction configurations used for household and pick-and-place scenarios. We adopt a server-client inference loop in which, at each timestep, the client captures the current RGB (or RGB-D) observations and proprioceptive states, packages them into a policy query, and sends the request to the inference server. The server processes this input through the GR00T policy and returns the predicted action, which is immediately applied to the simulator.

Model Configuration	PnP Can to Drawer Close	PnP Potato to Microwave Close	PnP Wine to Cabinet Close
GR00T N1.5 (Zero-shot)	18.0%	18.0%	15.0%
Standard Finetuning (Baseline)	51.0%	49.0%	46.0%
Ours (+ Contact State)	56.0%	51.0%	51.0%
Ours (+ Contact Encoder)	14.0%	15.0%	10.0%
Ours (+ Depth)	61.0%	49.0%	59.0%
Ours (+ Contact, + Depth)	63.0%	51.0%	61.0%

TABLE 1: Ablation study on modality augmentation conducted using the GR1 dataset released on HuggingFace.

Model Configuration	MSE (↓)
GR00T N1.5 (Zero-shot	0.054825
Standard Finetuning (Baseline)	0.021566
Ours (+ Contact State)	0.019662
Ours (+ Contact Encoder)	0.042569
Ours (+ Depth)	0.015234
Ours (+ Contact, + Depth)	0.011547

TABLE 2: Offline evaluation results (GT vs. MSE) for PnP Can to Drawer Close task

The success rate is computed as:

Success Rate = 
$$\frac{\text{# successful rollouts}}{\text{# total rollouts}}$$
.

For each task, we perform 20 randomized rollouts with varying initial object positions and robot configurations to evaluate robustness.

Complementary Nature of the Metrics.: Offline MSE captures the model's ability to match expert demonstrations but does not fully reflect closed-loop stability. Online evaluation measures actual manipulation success under embodiment-specific dynamics, noisy perceptual conditions, and contact-rich interactions. Together, these metrics provide a comprehensive assessment of policy quality across GR1 and G1 embodiments.

# C. GR1 Experiments: Modality Augmentation Analysis

We conduct a modality-wise ablation study on the publicly released GR1 dataset to evaluate the effect of contact and depth augmentation on both offline trajectory reconstruction and online manipulation performance.

- 1) Online Evaluation (Success Rate): Table 1 summarizes the online success rates measured through simulation rollouts across three GR1 tasks. Contact-state augmentation provides modest gains, while depth augmentation significantly improves success under visually ambiguous scenarios. The full model incorporating both depth and contact achieves the highest success rate across all evaluated tasks.
- 2) Offline Evaluation (MSE): Table 2 reports the meansquared error (MSE) between the predicted and groundtruth action trajectories for the PnP Can to Drawer Close task. Among all configurations, depth augmentation provides the most substantial improvement in offline reconstruction quality, indicating that geometric cues significantly reduce

ambiguity in action prediction. Furthermore, combining both depth and contact information yields the lowest overall error, demonstrating the complementary benefit of integrating multi-modal signals into the diffusion denoising process.

# D. G1 Experiments: Embodiment Transfer with Custom Multi-Modal Data

To assess embodiment transfer and quantify the impact of contact-rich demonstrations on the Unitree G1, we perform a modality ablation study on a customized *Pick Apple to Bowl* dataset generated using cuRobo-based motion planning and ground-truth force measurements. Compared to the GR1 platform, the G1 provides explicit 6-axis force sensing and a 7-DoF dexterous hand, offering a more informative testbed for analyzing how contact and geometric modalities contribute to fine-grained manipulation.

Model Configuration	Success Rate (%)	MSE
GR00T N1.5 (Zero-shot)	0.0%	0.35719
GR00T N1.5 (Finetuning)	48.0%	0.031716
Ours (+ Contact Encoder)	74.0%	0.024407
Ours (+ Contact State)	94.0%	0.018623
Ours (+ Depth)	82.0%	0.022596

TABLE I

Ablation study on multi-modal augmentation for  ${\small \mbox{\bf EMBODIMENT TRANSFER on Unitree $G1$}}.$ 

1) Online Evaluation (Success Rate): Table 1. reports the online evaluation results across all modality configurations. Zero-shot GR00T N1.5 fails entirely on the G1, underscoring the substantial embodiment gap between GR1 and G1 in hand morphology, sensor topology, and contact dynamics. Finetuning with 5K embodiment-aligned demonstrations im-

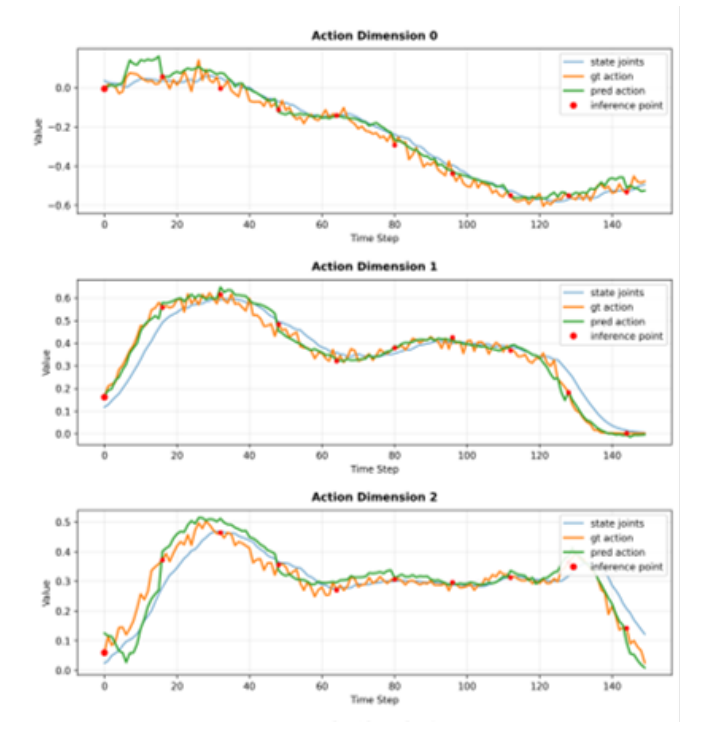


Fig. 8. Comparison between ground-truth actions, predicted actions, and executed inference points across the first three action dimensions. The model closely tracks the demonstration trajectory, indicating stable diffusion-based denoising and accurate action reconstruction.

proves performance to 48%, demonstrating that platform-specific data is essential for stable closed-loop control.

Incorporating contact-force measurements yields significant additional gains. Modeling force signals as an auxiliary modality increases success to 74%, indicating that contact cues provide valuable information for regulating grasp pressure and mitigating slip during the transport phase. The best performance (94%) arises when force signals are fused directly into the proprioceptive state representation, suggesting that early fusion produces richer latent dynamics and stronger conditioning for the diffusion-based denoising process.

Depth augmentation also contributes substantial improvements. Integrating depth features achieves an 82% success rate, showing that 3D geometry aids in resolving self-occlusion, disambiguating the apple–bowl interaction region, and stabilizing approach trajectories. However, unlike the GR1—where depth was the dominant performance factor due to limited contact sensing—the G1 benefits more from force-aware modalities. This indicates that depth alone cannot capture the fine-scale local interactions required for dexterous contact-rich manipulation.

Cross-Embodiment Insight.: Overall, the results highlight that optimal modality design is inherently embodimentspecific. GR1 derives most of its improvement from geometric augmentation, whereas G1 relies primarily on contact-rich supervision to compensate for its higher manipulation dexterity and increased interaction complexity. These findings underscore that successful transfer of foundation policies to new platforms requires aligning sensory modalities with the target robot's kinematic structure and physical interaction characteristics.

#### VI. CONCLUSION AND FUTURE WORK

This work presented a modality-augmented fine-tuning framework for adapting foundation robot policies to heterogeneous embodiments. Using the GR1 dataset, we showed that depth augmentation substantially improves both offline trajectory reconstruction and online manipulation success, while contact-state integration provides complementary gains for contact-rich tasks. To address the limitations of RGBonly public datasets, we introduced a customized multimodal dataset for the Unitree G1, generated using cuRobobased motion planning and ground-truth force measurements. Experiments demonstrate that contact-force supervision is essential for reliable control on the G1 platform: while zeroshot GR00T fails due to embodiment mismatch, incorporating contact information yields a dramatic performance increase, achieving up to 94% success in the Pick Apple to Bowl task.

Our cross-embodiment analysis highlights that optimal modality selection depends strongly on robot morphology and sensing capabilities: depth is most beneficial for the GR1's visually ambiguous manipulation scenes, whereas explicit contact-force feedback is crucial for the G1's dexterous hand and grasp-centric behaviors. These findings underscore the importance of tailoring modality design and dataset construction to the target embodiment when deploying foundation policies across platforms.

**Future Work.** There are several promising directions for extending this study. First, integrating real-world sensory streams—such as tactile arrays, joint torque measurements, and stereo depth—would enable evaluation beyond simulation and support robust sim-to-real deployment. Second, jointly training the vision, language, and diffusion modules, rather than relying on frozen VLM backbones, may lead to stronger multi-modal fusion and improved generalization. Third, expanding the G1 dataset to additional task families and more diverse environments would facilitate large-scale multi-embodiment benchmarking. Fourth, exploring crossrobot policy distillation or embodiment-conditioned latent representations may further improve transfer between morphologically distinct robots.

Another promising direction is the development of a contact-adaptive denoising schedule for diffusion policies. Prior to establishing contact, the policy could employ a larger number of denoising iterations with higher noise levels  $(\sigma_t)$  to encourage broader action exploration, improve wrist alignment, and mitigate approach-phase miscalibration. After contact is detected, the algorithm could transition to fewer iterations with lower  $\sigma_t$ , yielding a contact-conditioned  $\beta_t/\sigma_t$  schedule that stabilizes grasp execution and reduces action variance during transport. Such adaptive schedules may significantly improve closed-loop robustness in contact-rich manipulation.

Overall, our results demonstrate that modality-aware finetuning, combined with carefully constructed multi-modal datasets, provides an effective pathway for adapting foundation robot policies to new embodiments and unlocking robust manipulation capabilities across platforms.

#### REFERENCES

- [1] J. Ho, A. Jain, and P. Abbeel, "Denoising diffusion probabilistic models," in *Advances in Neural Information Processing Systems*, 2020.
- [2] J. Song, C. Meng, and S. Ermon, "Denoising diffusion implicit models," in *International Conference on Learning Representations*, 2021
- [3] W. Peebles and S. Xie, "Scalable diffusion models with transformers," in *Proceedings of the IEEE/CVF International Conference on Computer Vision*, 2023.
- [4] Y. Lipman et al., "Flow matching for generative modeling," in *International Conference on Learning Representations*, 2023.
- [5] J.-B. Alayrac et al., "Flamingo: A visual language model for fewshot learning," in Advances in Neural Information Processing Systems, 2022.
- [6] A. Brohan et al., "RT-2: Vision-language-action models transfer web knowledge to robotic control," Google DeepMind technical report, 2023.
- [7] P. Jain et al., "OpenVLA: An open vision-language-action model for generalist robots," Technical report, 2024.
- [8] T. Kollar et al., "Octo: An embodied foundation model for robotic manipulation," Technical report, 2024.
- [9] NVIDIA, "GR00T N1: An open foundation model for generalist humanoid robots," NVIDIA Research report, 2025.
- [10] Y. Xia et al., "PerAct: Perception-and-action transformers for robotic manipulation," in *Conference on Robot Learning*, 2022.
- [11] T. Chi et al., "Diffusion policy: Visuomotor policy learning via action diffusion," in *Robotics: Science and Systems*, 2023.
- [12] H. Jang et al., "Depth-aware policy learning for robot manipulation," in *IEEE International Conference on Robotics and Automation*, 2024.
- [13] R. Calandra et al., "Deep tactile representation learning," *International Journal of Robotics Research*, 2021.
- [14] A. Church et al., "Learning contact-rich manipulation with differentiable physics," in *Robotics: Science and Systems*, 2022.
- [15] A. Z. Wang et al., "robosuite: A modular simulation framework for robot learning," in *IEEE International Conference on Robotics and Automation*, 2020.
- [16] M. Li et al., "RoboCasa: Large-scale household simulation for robotic manipulation," Meta AI technical report, 2023.
- [17] P. Sundaram et al., "cuRobo: Parallelized motion generation for complex robotic systems," NVIDIA Research report, 2023.
- [18] D. Berenson et al., "Learning neural inverse kinematics solvers for articulated robots," in *IEEE International Conference on Robotics and Automation*, 2022.
- [19] S. Bhat et al., "ZoeDepth: Zero-shot metric monocular depth estimation," in *IEEE/CVF Conference on Computer Vision and Pattern Recognition*, 2023.
- [20] J. T. Wu et al., "EgoSchema: Scaling robot learning with egocentric multimodal data," Technical report, 2024.